Solution-Based Processing of the Phase-Change Material KSb_5S_8

David B. Mitzi,[†,*] Simone Raoux,[‡] Alex G. Schrott,[†] Matthew Copel,[†] Andrew Kellock,[‡] and Jean Jordan-Sweet[†]

IBM T. J. Watson Research Center, P.O. Box 218, Yorktown Heights, New York 10598, and IBM Almaden Research Center, 650 Harry Rd, San Jose, California 95120

Received August 18, 2006. Revised Manuscript Received October 20, 2006

A hydrazine-based process for solution-depositing phase-change materials (PCMs) is demonstrated, using KSb_5S_8 (KSS) as an example. The process involves dissolving the elemental metals and chalcogen in hydrazine at room temperature and spin-coating the solution onto a substrate, followed by a short low-temperature ($T \leq 250$ °C) anneal. The spin-coated KSS films, which range in thickness from 10 to 90 nm, are examined using variable temperature X-ray diffraction, medium energy ion scattering (MEIS), Rutherford backscattering spectroscopy (RBS), and scanning electron microscopy (SEM). The spin-coated KSS films exhibit a reversible amorphous-crystalline transition with a relatively high crystallization temperature (∼280 °C). Selected other chalcogenide-based PCMs are also expected to be suitable for thin-film deposition using this approach.

Introduction

Interest in phase-change materials (PCMs) has flourished recently, as a result of emerging technologies including, most notably, commercially available rewritable optical media (e.g., CD-RW, DVD-RW)[1−6] and the development of nonvolatile phase-change memory (PRAM).[7−9] Each of these applications employs a chalcogenide-based PCM film, which must be switchable between two physical states (i.e., usually amorphous and crystalline). The change in state of the PCM must also be detectable using a physical measurement, such as optical absorption, reflectivity, or electrical resistivity. As an example,[4−6] amorphous as-deposited $Ge_2Sb_2Te_5$ (GST) films may be converted to crystalline form using a laser to heat the material above the crystallization temperature. Exposure to a short, more intense laser pulse may then locally melt the crystallized GST resulting, upon quenching, in back conversion to a discrete amorphous mark on a crystalline background. The reversibility of the laser crystallization−amorphization process, as well as the detectable difference in optical properties between the amorphous and crystalline regions, enables the effective design of a rewritable optical memory. In addition to technological applications, PCMs also are of significant fundamental interest with respect to understanding the nature of the phase-change process (e.g., mechanism of the structural phase transition, factors limiting the crystallization rate, nature of the amorphous state).[5,6]

Numerous prospective Se- and Te-based PCMs have been examined for use in memory applications as well as for more fundamental studies including: In−Se,[8,10] In−Se−Tl,[11] Ga−Te−Se,[12] Sb−Se,[13] Sb−Se−Bi,[14] Sb−Te,[15] In−Sb−Te,[16] Ag−In−Sb−Te,[17] Sn−Te−Se,[18] Ge−Te,[3] Ge−Te−Sn,[19] Ge−Te−As,[2,20] Ge−Sb−Te,[4,21] and Ge−Sb−Te−Se.[22] Most of these systems (with the notable exception of Ge−Te, Ge−Sb−Te and Ag−In−Sb−Te) exhibit relatively long crystallization times (>200 ns), rendering them incompatible with

* Corresponding author. E-mail: dmitzi@us.ibm.com, fax: (914) 945-2141.
† IBM T. J. Watson Research Center.
‡ IBM Almaden Research Center.

(1) Feinleib, J.; de Neufville, J.; Moss, S. C.; Ovshinsky, S. R. *Appl. Phys. Lett.* **1971**, *18*, 254.
(2) von Gutfeld, R. J.; Chaudhari, P. *J. Appl. Phys.* **1972**, *43*, 4688.
(3) Chen, M.; Rubin, K. A.; Barton, R. W. *Appl. Phys. Lett.* **1986**, *49*, 502.
(4) (a) Ohta, T. *J. Optoelectron. Adv. Mater.* **2001**, *3*, 609; (b) Ohta, T.; Nishiuchi, K.; Narumi, K.; Kitaoka, Y.; Ishibashi, H.; Yamada, N.; Kozaki, T. *Jpn. J. Appl. Phys. (Pt. 1)* **2000**, *39*, 770.
(5) (a) Wełnic, W.; Pamungkas, A.; Detemple, R.; Steimer, C.; Blügel, S.; Wuttig, M. *Nature Mater.* **2006**, *5*, 56; (b) Kolobov, A.; Fons, P.; Frenkel, A. I.; Ankudinov, A. L.; Tominaga, J.; Uruga, T. *Nature Mater.* **2004**, *3*, 703.
(6) Zhou, G.-F. *Mater. Sci. Eng. A* **2001**, *73*, 304−306.
(7) Ovshinsky, S. R. *J. Non-Cryst. Solids* **1970**, *2*, 99.
(8) Lee, H.; Kim, Y. K.; Kim, D.; Kang, D.-H. *IEEE Trans. Magn.* **2005**, *41*, 1034.
(9) Oh, H. et. al. *IEEE J. Solid-State Circuits* **2006**, *41*, 122.
(10) Terao, M.; Nishida, T.; Miyauchi, Y.; Horigome, S.; Kaku, T.; Ohta, N. *Proc. SPIE-Int. Soc. Opt. Eng.* **1986**, *695*, 105.
(11) Nishida, T.; Terao, M.; Miyauchi, Y.; Horigome, S.; Kaku, T.; Ohta, N. *Appl. Phys. Lett.* **1987**, *50*, 667.
(12) Matsushita, T.; Suzuki, A.; Okuda, M.; Rhee, J. C.; Naito, H. *Jpn. J. Appl. Phys.* **1985**, *24*, L504.
(13) Barton, R.; Davis, C. R.; Rubin, K.; Lim, G. *Appl. Phys. Lett.* **1986**, *48*, 1255.
(14) Ishigaki, M.; Tokushuku, N.; Ohishi, T.; Kodera, Y.; Ohta, Y.; Fukui, Y. *Proc. SPIE-Int. Soc. Opt. Eng.* **1986**, *695*, 99.
(15) Yagi, S.; Fujimori, S.; Yamazaki, H. *Jpn. J. Appl. Phys.* **1987**, *26* (Supplement 26-4.; Proceedings of the International Sympsium on Optical Memory), 51.
(16) Maeda, Y.; Andoh, H.; Ikuta, I.; Minemura, H. *J. Appl. Phys.* **1988**, *64*, 1715.
(17) Iwasaki, H.; Harigaya, M.; Nonoyama, O.; Kageyama, Y.; Takahashi, M.; Yamada, K.; Deguchi, H.; Ide, Y. *Jpn. J. Appl. Phys.* **1993**, *32*, 5241.
(18) Terao, M.; Nishida, T.; Miyauchi, Y.; Nakao, T.; Kaku, T.; Horigome, S.; Ojima, M.; Tsunoda, Y.; Sugita, Y. *Proc. SPIE* **1985**, *529*, 46.
(19) Chen, M.; Rubin, K. A.; Marrello, V.; Gerber, U. G.; Jipson, V. B. *Appl. Phys. Lett.* **1985**, *46*, 734.
(20) Smith, A. W. *Appl. Opt.* **1974**, *13*, 795.
(21) Yamada, N.; Ohno, E.; Nishiuchi, K.; Akahira, N.; Takao, M. *J. Appl. Phys.* **1991**, *69*, 2849.
(22) (a) Coombs, J. H.; Jongenelis, A. P. J. M.; van Es-Spiekman, W.; Jacobs, B. A. J. *J. Appl. Phys.* **1995**, *78*, 4906; (b) Coombs, J. H.; Jongenelis, A. P. J. M.; van Es-Spiekman, W.; Jacobs, B. A. J. *J. Appl. Phys.* **1995**, *78*, 4918.

10.1021/cm0619510 CCC: $33.50
Published on Web 12/19/2006

high data-transfer-rate operation in rewritable electronic and optical applications.[6] Besides a propensity for glass formation during melt-quenching and fast recrystallization upon heating, other desirable criteria for PCMs include sufficient contrast in physical properties between the crystalline and amorphous states, a relatively high crystallization temperature (preferably >150 °C for thermal stability considerations), excellent cycling properties (for repeated write-erase cycles), and high resistivity in the crystalline phase coupled with relatively low melting point (preferably <600 °C) for application in solid-state memory devices (to minimize the RESET and SET currents).[6] Recently, an unusual sulfur-based PCM, KSb_5S_8 (KSS), has been reported.[23,24] Unlike many chalcogenide glasses, KSS is a congruently melting stoichiometric compound, with a higher glass-to-crystallization temperature than GST (287 °C) and a coexistence of ionic and covalent bonding within the compound (most other PCMs have primarily covalent bonding).[23] In addition, KSS provides a relatively large optical band gap (i.e., 1.82 eV for crystalline and 1.67 eV for glass forms) compared with GST, suggesting possible utility in high-density optical data storage applications using short wavelength laser beams.[23]

Along with materials issues, fabrication cost considerations are critical for the success of any potential PCM technology. Thin film deposition is crucial both for PCM applications, as well as for more basic studies. Generally, PCM films are deposited using vacuum-based techniques such as sputtering or thermal evaporation.[2,8,11,13,16,17,19−22] A low-temperature solution-based process would be desirable because of the reduced complexity and cost of the process (e.g., no vacuum requirements), the possibility of higher film-processing throughput, and the ability to deposit on a wider range of substrate types and surface morphologies (including substrates that have a very large area and/or are flexible). In this study, we demonstrate the application of the hydrazine-precursor technique[25−30] to the low-temperature (T < 250 °C) solution-based processing of PCMs (bulk and thin-film form), using KSS as an example, and also examine the phase-change characteristics of the resulting KSS films using variable-temperature X-ray diffraction. The ability to deposit thin films of KSS enables a comparison with earlier studies on bulk KSS materials prepared by a high temperature (>800 °C) solid-state technique.[23] Additionally, in contrast to our previous studies on the hydrazine-precursor technique,[25−30] we also demonstrate that precursor solution preparation can be achieved by dissolving the appropriate elemental metals and chalcogen in the hydrazine solvent at room temperature, rather than by employing preformed metal chalcogenides as starting materials.

(23) Kyratsi, T.; Chrissafis, K.; Wachter, J.; Paraskevopoulos, K. M.; Kanatzidis, M. G. *Adv. Mater.* **2003**, *15*, 1428.
(24) Chrissafis, K.; Kyratsi, T.; Paraskevopoulos, K. M.; Kanatzidis, M. G. *Chem. Mater.* **2004**, *16*, 1932.
(25) Mitzi, D. B.; Kosbar, L. L.; Murray, C. E.; Copel, M.; Afzali, A. *Nature* **2004**, *428*, 299.
(26) Mitzi, D. B.; Copel, M.; Chey, S. J. *Adv. Mater.* **2005**, *17*, 1285.
(27) Milliron, D. J.; Mitzi, D. B.; Copel, M.; Murray, C. E. *Chem. Mater.* **2006**, *18*, 587.
(28) Mitzi, D. B.; Copel, M.; Murray, C. E. *Adv. Mater.* **2006**, *18*, 2448.
(29) Mitzi, D. B. *Inorg. Chem.* **2005**, *44*, 7078.
(30) Mitzi, D. B. *Inorg. Chem.* **2005**, *44*, 3755.

Experimental Section

Synthesis. Under rigorously inert atmosphere conditions, 0.5 mmol of elemental K (19.6 mg; Alfa Aesar, 99.95%, ampouled under Ar) is combined with 2.5 mmol of Sb (304.4 mg; Alfa Aesar; 99.999%, −200 mesh), 8.0 mmol of S (256.5 mg; Aldrich, 99.998%), and 1.0 mL of anhydrous distilled hydrazine. **NOTE: Hydrazine is highly toxic and should be handled using appropriate protective equipment to prevent contact with either the vapors or liquid.** The hydrazine must be added carefully (drop-by-drop and very slowly) to accommodate the highly exothermic reaction. One method to overcome the highly exothermic nature of the reaction between potassium and hydrazine is to have the potassium physically removed from the bottom of the reaction vessel (e.g., K is "sticky" at room temperature and will effectively stick to the side of the glass walls of the reaction flask). When the hydrazine drops are placed on the bottom of the reaction flask, the vapors can first be allowed to react with the K on the side wall, followed by gentle agitation of the vessel, allowing some of the drop to gradually come into direct contact with the remaining K. The mixture is stirred for several days at room temperature in a nitrogen-filled drybox, forming an essentially clear relatively viscous yellow solution (a tiny amount of black precipitate or undissolved material is still present but can be easily removed using a filter). For bulk analysis of the precursor, the filtered solution was evaporated under flowing nitrogen gas and under vacuum, yielding a very viscous darkly colored gum-like product.

In analogy with the reaction of other metal chalcogenides and S/Se in hydrazine,[25−28,30] and considering the starting charge composition, we expect a composition $(N_2H_4)_y(N_2H_5)_{2x}KSb_5S_{8+x}$ for the final bulk precursor. Chemical analysis of the product (performed by Galbraith Laboratories, Knoxville, TN) yielded: N 21.9(5)%, H 3.5(5)%. These results, coupled with the weight loss exhibited upon thermal decomposition to KSb_5S_8 (36.4%, see Figure 1), indicate an approximate composition $(N_2H_4)_{1.7}(N_2H_5)_{9.4}KSb_5S_{12.7}$ (i.e., the weight loss and chemical analysis experiments yield two independent equations for x and y, which can be solved, yielding, $x \approx 4.7$, $y \approx 1.7$). Note that the nominally amorphous nature of the product precludes most crystallographic X-ray structure analysis. Given the relatively indirect determination of the stoichiometry, the proposed chemical composition should be viewed as approximate pending more complete chemical evaluation. In addition, the exact chemical composition of the bulk precursor depends significantly on the extent of drying to which the precursor is subjected (i.e., hydrazine is readily lost at room temperature).

Thin-Film Deposition. For thin-film deposition, the above-described solution proved too viscous for effective deposition by spin-coating. The solution was therefore diluted by adding an additional 3−9 mL of distilled hydrazine (~0.12−0.05 M with respect to KSb_5S_8 content). The different concentrations were chosen to target selected film thicknesses. Films could then be spin-coated from the hydrazine-based solution onto thermal-oxide-coated Si substrates (2 cm × 2 cm), which had been cleaned using a Piranha process (4:1 H_2SO_4: 30% H_2O_2 by volume). The films were spin-coated in a nitrogen-filled drybox by depositing two drops of the precursor solution on the substrate and spin-coating at the final rotational speed of 2500−5000 rpm (again depending on targeted deposition thickness) for 60 s. After being spin-coated, the resulting films were dried at 125 °C for approximately 5 min and then gradually heated to 250 °C over a period of 80 min and maintained at this temperature for 10 min. This heat treatment decomposes the precursor, resulting in the desired KSb_5S_8 films.

X-ray Diffraction. Bulk XRD patterns were collected at room-temperature using a Siemens D5000 diffractometer (Cu Kα radiation). Thin-film samples were prepared as described above.

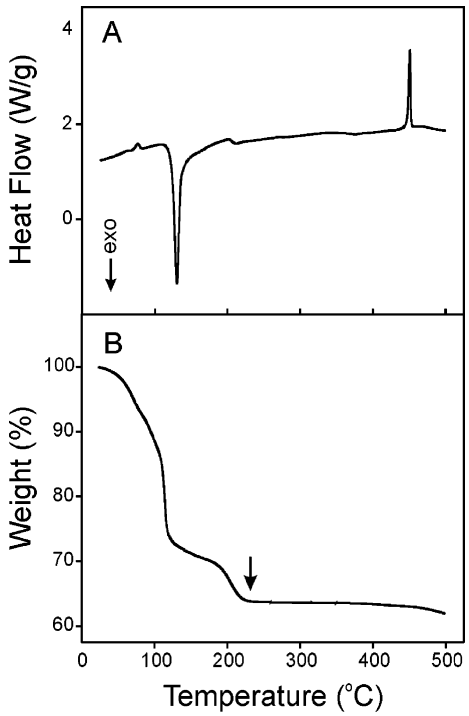

Figure 1. (A) Differential scanning calorimetry (DSC) scan for the KSb_5S_8 precursor (5 °C/min ramp rate). Exothermal peaks are down along the heat flow axis. (B) Thermogravimetric analysis (TGA) for the KSb_5S_8 precursor (1 °C/min ramp rate). The arrow in the TGA plot highlights the highest temperature to which the precursor was heated (before cooling) in preparation for the X-ray diffraction experiment depicted in Figure 2.

Time-resolved *in situ* XRD experiments were performed on the films at beamline X-20C of the National Synchrotron Light Source using a photon energy of 6.9 keV ($\lambda = 1.797$ Å). The setup consisted of a high-throughput synthetic multilayer monochromator and fast linear-diode-array detector. The films were heated *in situ* using a BN heater, capable of rapid annealing up to 1100 °C at a rate of ≤35 °C/s in an atmosphere of purified He. The phase(s) present in each sample (bulk and thin-film) were identified by comparison with powder diffraction file (PDF) cards and, in the case of KSb_5S_8, by comparison with the calculated powder patterns from the single-crystal structure.[31] In this latter case, the powder patterns were generated using the Mercury (v.1.3) program[32] using either $\lambda = 1.54$ Å or $\lambda = 1.797$ Å.

Other Characterization. Thermogravimetric analysis **(**TGA) scans were performed, using a TA Instruments TGA-2950 system, in a flowing nitrogen atmosphere and with a 1 °C/min ramp to 500 °C. Differential scanning calorimetry (DSC) thermograms were collected on a TA Instruments MDSC-2920 under a nitrogen purge and using a 5 °C/min temperature ramp rate. The aluminum sample pans for the DSC measurement were sealed with a top lid. However, a small hole was punched into the lid to allow the decomposition products (evolved gases) to escape from the container.

Medium energy ion scattering (MEIS) analysis[33] was performed, to determine chemical composition and thickness of the thin films, with 200 keV protons using an electrostatic energy analyzer at a scattering angle of 120°. The system was calibrated to better than 5% accuracy using a SiO_2 film of known thickness. For thicker films, Rutherford backscattering spectrometry (RBS) was used to establish composition and thickness. The RBS measurements were performed with 2.3 MeV He^+ ions using an NEC 3UH Pelletron. Spectra were collected at 170° to maximize peak separation of the K and S signals. The composition was determined with an uncertainty of 0.5 atom %, and the film thickness was measured with an accuracy of 5%. The N and H concentrations for the spin-coated KSS films were checked by RBS and found to be less than a few percent.

Scanning electron microscopy (SEM) measurements were performed on the KSS-coated substrates, prepared under various conditions (as described above). The coated substrates were cleaved prior to the SEM analyses and coated with a thin Pd−Au film to prevent charging effects. The images were taken at a 15° tilt, so that both the top surface and the exposed chalcogenide-SiO_2 interface could be simultaneously viewed. Using the cross-sectional SEM images, the thicknesses of films deposited using the various above-described preparation conditions were determined and are in agreement with the thickness values achieved using either MEIS or RBS.

Results and Discussion

Metal chalcogenides, $A_qM_nX_m$, where M is a metal or mixture of metals, X is a chalcogen or mixture of chalcogens, and A is an optional alkali metal component, are often formed using high-temperature (energy-intensive) and/or multistep (time-consuming) reactions.[23,24,34,35] As an example, bulk KSS is generally prepared by either heating a stoichiometric combination of K, Sb, and S at 850 °C or by reaction of KNO_3, S, and $KSb(OH)_6$ under hydrothermal conditions.[23,31] The latter hydrothermal approach does not yield a single-phase product (significant inpurity phase of $KSbS_2$).[31] KBi_2CuS_4, $A_3Bi_5Cu_2S_{10}$, $A_2Hg_3Q_4$, $A_2Hg_6Q_7$ (A = K, Rb, Cs; Q = S, Se) and related compounds are each formed by first preparing the alkali metal chalcogenide A_2Q_n ($n = 1$ or 3) in a liquid ammonia media, followed by reaction of this component with the other metal chalcogenides or component elements and chalcogens at temperatures ranging from 220−850 °C.[34,35] The reaction products using this approach also often contain secondary phases, in addition to the targeted composition.

In the current study, the KSS precursor solution was prepared by carefully (see Experimental Section) dissolving elemental potassium, antimony, and sulfur in hydrazine under an inert atmosphere. The ability to prepare the KSS solution at ambient temperature in a single vessel from the elements, without the need to first isolate the metal chalcogenide, represents an alternative to the previously described hydrazine precursor process[25−30] and has been further demonstrated with several other related binary chalcogenide systems (e.g., SnS_2, In_2Te_3, Ga_2Se_3). To examine the properties of the bulk KSS precursor, hydrazine was evaporated from the precursor solution, yielding a gum-like product with approximate chemical composition (determined from chemical and thermal analysis) of $(N_2H_4)_{1.7}(N_2H_5)_{9.4}KSb_5S_{12.7}$. As seen in Figures 1A and 1B, the KSS precursor decomposes exothermally ($\Delta H = \sim 430$ J/g) beginning near ~124 °C (exact temperature depends on heating rate), with a smaller endo-

(31) Berlepsch, P.; Miletich, R.; Armbruster, T. *Z. Kristallogr.* **1999**, *214*, 57.
(32) Bruno, I. J.; Cole, J. C.; Edgington, P. R.; Kessler, M.; Macrae, C. F.; McCabe, P.; Pearson, J.; Taylor, R. *Acta Crystallogr.* **2002**, *B58*, 389.
(33) Van der Veen, J. F. *Surface Sci. Rep.* **1985**, *5*, 199.
(34) Axtell, E. A., III; Park, Y.; Chondroudis, K.; Kanatzidis, M. G. *J. Am. Chem. Soc.* **1998**, *120*, 124.
(35) Yang, Y.; Brazis, P.; Kannewurf, C. R.; Ibers, J. A. *J. Solid State Chem.* **2000**, *155*, 243.

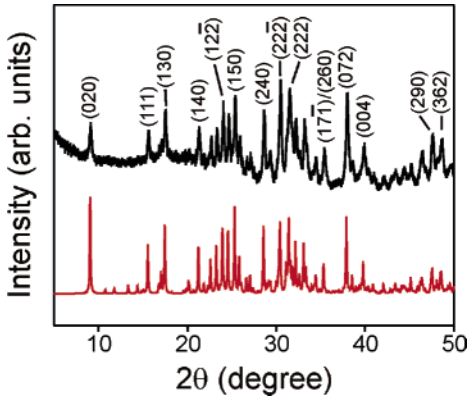

Figure 2. Powder X-ray diffraction data from the precursor after a TGA run terminated at 230 °C (top black curve), acquired using Cu Kα radiation (λ = 1.54 Å) and demonstrating good agreement with the simulated diffraction pattern for bulk KSb_5S_8 (bottom red curve).[31] Selected reflection indices are indicated above the experimental curve. The cell parameters for the simulated pattern are *Pn*: a = 8.1374 Å, b = 19.5013 Å, c = 9.0620 Å, β = 91.932°.

thermal process also noted at ~70 °C (perhaps related to a structural transition and/or dissociation of the neutral hydrazine). The observed weight loss of 36.4% at 300 °C during the multistep decomposition process corresponds to the loss of hydrazine and hydrogen sulfide (or their decomposition products) from the KSb_5S_8 precursor and is essentially complete by 230 °C. Remarkably, the X-ray diffraction pattern of the product formed by decomposing the precursor at this low temperature matches that expected for bulk KSS (Figure 2).[31] Rather than requiring a temperature of ~850 °C for more traditional high-temperature KSS preparation[23,24] or hydrothermal conditions,[31] the hydrazine-precursor approach provides a low-temperature, ambient-pressure synthetic pathway to single-phase bulk KSS. Note that the temperature of the melting endotherm with onset at 448(2) °C (Figure 1A) corresponds closely with that observed previously for bulk KSS prepared using the high-temperature route.[23] Additionally, the thermogravimetric analysis (TGA) data suggest a slight mass loss at temperatures approaching and above the melting point, either as a consequence of evaporation of the KSS material or of slow decomposition, resulting in slight changes in stoichiometry.

Films are formed by spin-coating the precursor solution onto thermally oxidized silicon substrates and then performing a short decomposition step with a maximum temperature of ~250 °C. The resulting composition and thickness for spin-coated films (prepared as described in the Experimental Section using a 0.05 M precursor solution and 4000 rpm spin speed) are $K_{1.2(1)}Sb_{4.9(1)}S_{8.0(1)}$ and 20.5(1) nm, respectively, as determined by medium-energy ion scattering (MEIS).[33] A very thin (~1.8 nm) sulfur-deficient (perhaps oxidized) surface layer is also indicated from the MEIS data modeling. Films with thicknesses ranging from ~10−90 nm have been successfully deposited using this process by changing solution concentration and spin speed. As an example, films spun using a 0.12 M precursor solution at 5000 rpm yielded films with composition $K_{1.1(1)}Sb_{4.9(1)}S_{8.0(1)}$ and average thickness 72(3) nm, as determined using Rutherford backscattering spectrometry (RBS). Changing the spin speed to 2500 rpm for the same solution produced

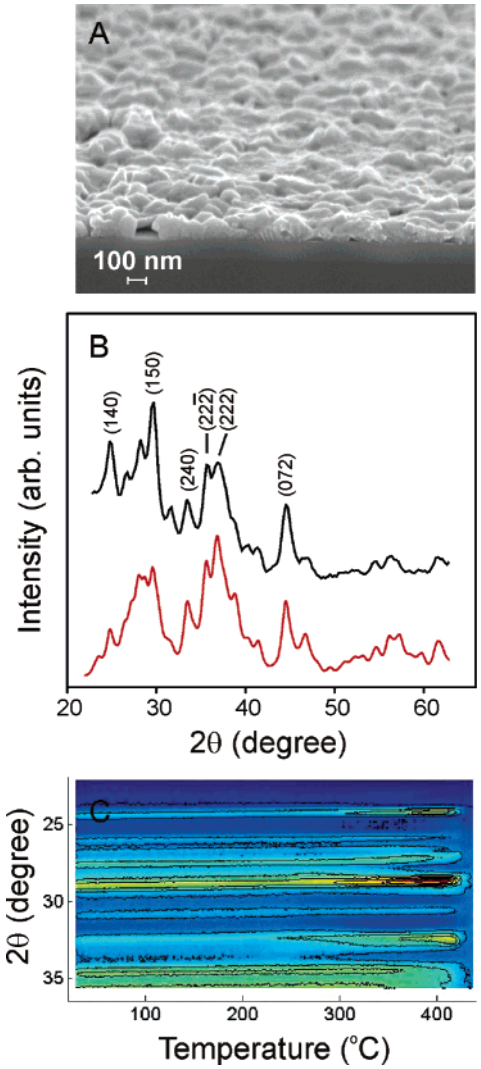

Figure 3. (A) Cross-sectional SEM of a spin-coated KSS film, prepared using a 0.12 M precursor solution with 2500 rpm spin speed and deposited on silicon coated with ~100 nm of thermal SiO_x. (B) X-ray diffraction (λ = 1.797 Å) from a spin-coated KSS film (top black curve), prepared using a 0.12 M precursor solution with 5000 rpm spin speed, demonstrating good agreement with the simulated pattern (bottom red curve; using 1° peak fwhm) for bulk KSS.[31] (C) Temperature-dependent X-ray diffraction (λ = 1.797 Å), using the same film as in Figure 3B. Peaks are indicated by deviation of the color from blue (background). Disappearance of the diffraction above 440(5) °C corresponds to the film melting.

thicker films (~91 nm). For single-coating depositions targeting thicknesses substantially in excess of 90 nm, deposited films generally delaminated from the substrate during the thermal decomposition step. However, thicker film deposition might be possible using multiple deposition/decomposition cycles (targeting relatively thin deposits each cycle).[27] Film surface roughness (see SEM image in Figure 3A) appears to be somewhat greater than that observed for the $SnS_{2-x}Se_x$ films and other previously deposited metal chalcogenides on the SiO_x surface,[25−30] perhaps because of grain growth during the highly exothermic decomposition or because of less favorable wetting characteristics for the KSb_5S_8 solutions relative to those for other examined chalcogenide systems. X-ray diffraction from the as-deposited films confirms that they are of the same phase as bulk KSS,[31] with little preferred orientation (Figure 3B). The diffraction peaks effectively disappear above ~440(5) °C (Figure 3C),

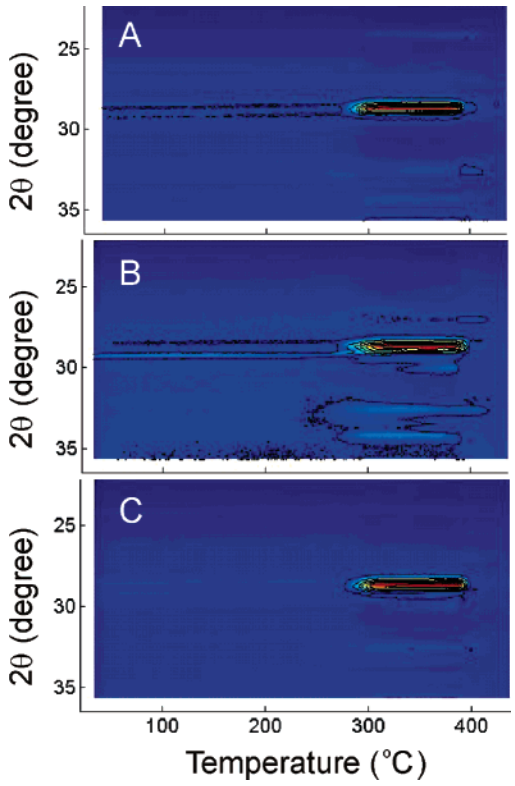

Figure 4. Three (A, B, C) sequential variable-temperature X-ray scans (λ = 1.797 Å) performed on the same spin-coated KSS film from Figure 3C after an initial heat and quench treatment. In each case, the heating rate is 1 °C/s and the sample is quenched to room temperature at the end of the heating portion of the cycle. Note the substantial degree of preferred orientation in the recrystallized film, with the (150) reflection dominating the observed diffraction pattern (compare with Figure 3C).

consistent with the expected melting temperature for KSb_5S_8.[23,24]

Quenching the KSS film used in the heating experiment of Figure 3C from above the melting temperature (460 °C to below 100 °C in ~1 min) leads to a nominally amorphous film. Interestingly, KSS films are much easier to melt quench than most PCMs. Other phase-change materials, such as GST, crystallize in times as short as tens of nanoseconds and thus require cooling rates of as high as 10^9 to 10^{10} °C/s in order to achieve an amorphous state.[21,36] The fact that bulk[23] and thin film KSS is relatively easy to quench into a glass, even using a relatively slow cool from the melt, suggests that the crystallization process in KSS may actually be relatively slow, contrary to the predictions based on DSC measurements.[23,24] Note, however, that a moderately slow crystallization rate does not preclude the use of a PCM in selected memory applications, especially those where the number of write cycles is relatively limited such as ROM (read-only memory) or WORM (write-once read-many) media.[37]

Subsequent heating of the amorphous KSS film at 1 °C/s leads to crystallization at ~280(5) °C (Figure 4A), in good agreement with the expected transition at 287 °C.[23] Further heating above 400 °C leads to remelting of the film. Three thermal cycles are shown in Figures 4A−C, demonstrating the reversibility of the amorphous-to-crystalline transition. Interestingly, after the first melting process, the subsequent melting transitions appear to shift to a lower temperature than for the initial melt, perhaps as a result of slight changes in the film stoichiometry above the melting point (as suggested by the TGA data). Compositional changes associated with evaporation or decomposition during heating in phase-change devices can often be alleviated using an encapsulation layer.[8]

Conclusion

In summary, we provide the first example of a solution-deposition process for chalcogenide-based PCMs, which is achieved using the hydrazine-precursor route.[25−30] Unlike closed vapor-deposition processes, high quality sputter targets or evaporation sources and a high vacuum environment are not required. While there are often difficulties encountered for vapor-phase deposition processes with regard to controlling film stoichiometry (e.g., different sticking coefficients or volatilities for the different elements in the compound, preferential sputtering, etc.), control over film composition can readily be achieved using the solution-based process. Assuming the absence of high temperature heat treatments, the metal stoichiometry of the solution directly translates to the metal content of the final film. Deposition rates can be very high for the solution-deposition process, and film thickness can be controlled via modifying the starting solution concentration and other solution-deposition parameters (i.e., spin speed for the spin-coating process).

For the KSS films considered in the current study, a repeatable amorphous-to-crystalline transition was demonstrated, with a reasonably high crystallization temperature (~280 °C). Additional studies are required to address the crystallization rate in the KSS films, which is an important characteristic to establish potential suitability for various memory applications, as well as to consider whether changes in stoichiometry (either within the K−Sb−S phase diagram or through addition of other elements) and/or tuning of film thickness or interface (or capping) layer can influence the crystallization kinetics, as has been observed in other PCMs.[6,21,38] For example, in the In_xSe_y system (deposited by traditional techniques), the crystallization time can be reduced by over 2 orders of magnitude by adjusting the stoichiometry and by incorporating Tl and Co.[38] Additionally, while we have demonstrated the spin-coating technique for KSS, we expect this process to be more generally applicable to the film deposition and bulk preparation of selected other chalcogenide-based PCMs.

Acknowledgment. The authors would like to thank R. M. Shelby for useful discussions regarding this work.

CM0619510

(36) Khulbe, P. K.; Wright, E. M.; Mansuripur, M. *J. Appl. Phys.* **2000**, *88*, 3926.
(37) Fischer, G. M.; Medower, B.; Revay, R.; Mansuripur, M. *Appl. Opt.* **2002**, *41*, 1998.
(38) Nishida, T.; Terao, M.; Nakazawa, M. *Jpn. J. Appl. Phys.* **1987**, *26* (Supplement 26−4.; Proc. Int. Symp. on Optical Memory), 67.